JOURNAL OF APPLIED ELECTROCHEMISTRY 20 (1990) 307–318

Ohmic drop and zones of reduced overpotential during the growth of small clusters

A. MILCHEV

Institute of Physical Chemistry, Bulgarian Academy of Sciences, 1040 Sofia, Bulgaria

Received 14 December 1988; revised 17 May 1989

The electrochemical growth of small clusters at constant external voltage has been studied theoretically. Expressions are derived here for the time dependence of the cluster size and the growth current accounting for the ohmic drop in the electrolyte. The potential distribution around the growing clusters is determined and the kinetics of spread of the zones of reduced overpotential are investigated.

1. Introduction

The electrochemical growth of microclusters has been extensively studied both experimentally and from a theoretical point of view [1–12]. Various growth mechanisms have been considered and theoretical expressions have been derived for the current–time relationship assuming different rate determining steps of the growth process. Thus it has been found that the ion transfer across the electrical double layer limits the growth of small clusters at short times whereas, for sufficiently large clusters, mass transport becomes the rate determining step. Mixed kinetics have also been considered [11].

It is the aim of this study to supplement the theory by accounting for the electrochemical ohmic drop which modifies the local electric field around the growing stable clusters. As is known the effect of the ohmic drop is often neglected for small clusters and therefore it is important to know up to what cluster size such an approximation is justified.

In this paper we consider the growth kinetics in concentrated well stirred solutions, in the absence of supporting electrolyte. Under such conditions the concentration of the electroactive species close to the growing clusters is almost equal to their bulk concentration and the concentration polarization is negligibly small. We consider this particular case for two reasons: first, to illustrate the pure effect of the ohmic drop on the ion transfer kinetics and, secondly, because the above mentioned conditions are close to the deposition conditions of corrosion-protective galvanic coatings.

2. Theory

2.1. *Basic kinetic equations*

The thermodynamic driving force for ion transfer across the electrical double layer is the electrochemical supersaturation $\Delta\mu$

$$\Delta\mu = ze\eta$$

In this expression z is the valency of the depositing ions, e is the elementary electric charge and η is the overpotential. The quantity $\Delta\mu$ determines the rate of the interfacial ion transfer reaction and enters the general theoretical expressions for the cathodic (I_c) and the anodic (I_a) current densities

$$I_c = i_0 \exp\left[\frac{\alpha ze\eta}{kT}\right] \quad (1)$$

$$I_a = i_0 \exp\left[-\frac{(1-\alpha)ze\eta}{kT}\right] \quad (2)$$

(Here, and throughout the paper, we define I_c and η as positive quantities.) In Equations 1 and 2, i_0 is the exchange current density (the crystal surface is considered as homogeneous with respect to the ion transfer process), α is the transfer coefficient and the other symbols have their usual meanings.

An essential problem in all experimental studies of electrochemical phase formation is the control and measurement of the overpotential, η. The main difficulty is because even in the case of growth at a fixed external voltage, ΔE, the actual overpotential at the cluster–solution interface may be not a constant but a time-dependent quantity. To make this point clear let us consider a two-electrode electrochemical cell comprising an electrolytic solution of metal ions, an inert ideally polarizable working electrode and an ideally non-polarizable counter electrode made of the metal whose ions are present in the solution. When applying an external voltage, ΔE, to the electrodes of such an electrochemical cell the process that proceeds first is the charging of the electrical double layer. During this process the electrochemical overpotential, η, is a function of time and changes according to

$$\eta(t) = \Delta E\,[1 - \exp(-t/\Omega C)] \quad (3)$$

where C is the double layer capacitance and Ω is the ohmic resistance of the electrolyte, which depends on the geometry of the electrolytic cell. Equation 3 shows that after time $t \approx 5\Omega C$ the double layer is almost fully charged and η becomes equal to the external voltage ΔE.

The appearance of a single growing cluster of the

0021-891X/90 $03.00 + .12 © 1990 Chapman and Hall Ltd.

new phase on the electrode surface is equivalent to a local breakdown of the double layer condenser and causes a partial decrease of the overpotential, η. Thus, at the cluster surface the overpotential becomes

$$\eta_r = \Delta E - iR_{\Omega,r} \tag{4}$$

where r is the cluster size, i is the growth current and $R_{\Omega,r}$ is the individual ohmic resistance of the circuit 'counter electrode–electrolyte–r-sized growing cluster'. (The Gibbs–Thomson effect of the curvature [7, 13, 14] is neglected in these considerations. An expression similar to Equation 4 is used in [29].) It is now η_r that ensures the ion transfer across the double layer to the cluster surface and, therefore, bearing in mind Equations 1 and 2 for the net growth current of the single cluster we obtain

$$i = S_r i_0 \left\{ \exp\left[\frac{\alpha z e \eta_r}{kT}\right] - \exp\left[-\frac{(1-\alpha) z e \eta_r}{kT}\right] \right\} \tag{5}$$

where S_r is the cluster surface area. To obtain the explicit i–r relationship, it is first necessary to define the quantities S_r and $R_{\Omega,r}$. For the sake of simplicity in the following we consider cap-shaped clusters formed on a flat working electrode (Fig. 1), γ being the contact angle betwen the cluster and the substrate. In this case $S_r = 4\pi r^2 \psi(\gamma)$, where $\psi(\gamma) = \frac{1}{2}(1 - \cos\gamma)$. $R_{\Omega,r}$ is not easy to find in the case of an arbitrary contact angle γ. However, for hemispherical clusters ($\gamma = 90°$) a solution can be obtained in the following way [2].

The ohmic resistance of the elctrolyte between two imaginary hemispheres with radii x' and $x' + \mathrm{d}x'$ (Fig. 2) is

$$\mathrm{d}R = \frac{1}{k_e} \frac{\mathrm{d}x'}{2\pi x'^2} \tag{6}$$

where k_e is the specific solution conductivity. Hence the ohmic resistance of the electrolyte between the r-sized cluster and a hemisphere with an arbitrary radius x is

$$R(x) = \int_r^x \frac{\mathrm{d}x'}{2\pi k_e x'^2} = \frac{1}{2\pi k_e r}\left(1 - \frac{r}{x}\right) \tag{7}$$

Therefore, if the distance between the cluster and the counter electrode is $x = L \gg r$ for the total ohmic resistance of the circuit 'counter electrode–electrolyte–r-sized cluster' one obtains

$$R_{\Omega,r} = \frac{1}{2\pi k_e r}\left(1 - \frac{r}{L}\right) \approx \frac{1}{2\pi k_e r} \tag{8}$$

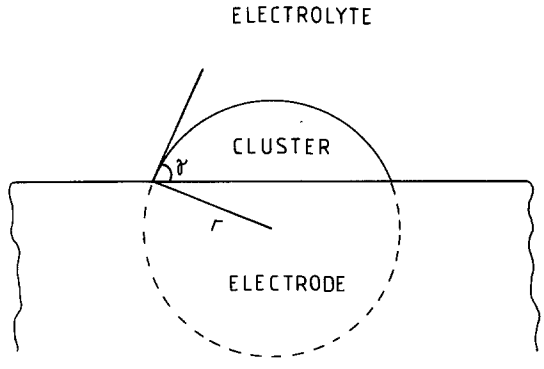

Fig. 1. Cap-shaped cluster of radius r and wetting angle γ.

For the case of an arbitrary contact angle, γ, the ohmic resistance can be approximately determined from Equation 7 if the integration is performed from an effective radius $r_{\mathrm{eff}} = fr$ [6]. Thus for $R(x)$ and $R_{\Omega,r}$

$$R(x) = \frac{1}{2\pi f k_e r}\left(1 - \frac{fr}{x}\right) \tag{7'}$$

$$R_{\Omega,r} = \frac{1}{2\pi f k_e r}\left(1 - \frac{fr}{L}\right) \approx \frac{1}{2\pi f k_e r} \tag{8'}$$

where the dimensionless constant f is introduced to account for the complicated symmetry of the electric field arising around an arbitrary cap-shaped cluster of the new phase. As is seen from Equations 7′ and 8′ the correction appears in the form of an effective conductivity fk_e, different from the actual specific conductivity of the electrolytic solution. It is worth noting that, according to Lorenz [15], k_e must also be corrected in a similar way in the case of hemispherical clusters to take into account the increased surface conductivity of the electrolyte due to the higher concentration of metal ions in the region of the electrical double layer. All this means that the constant f has a rather complicated physical meaning and should be empirically determined in each particular experimental system.

Equations 7 and 7′ give the ohmic resistance $R(x)$ as a function of the distance x from the growing cluster and show that almost 90% of the total ohmic resistance $R_{\Omega,r}$ is concentrated in a layer with a thickness of about 10 cluster radii. Indeed for $x = 10r$ it follows from Equations 7 and 8 that $R(x) = 0.9\ R_{\Omega,r}$. This means that it is worth using a three-electrode system for decreasing the ohmic drop only if the tip of the Luggin capillary can be fixed to the growing cluster surface at a distance shorter than 10 times the cluster radius. Certainly this is impossible for clusters of size $r < 10^{-3}$ cm. For such clusters the effect of the ohmic drop should be either neglected or accounted for theoretically.

Returning to Equation 5 and substituting η_r by $(\Delta E - i/2\pi f k_e r)$ and S_r by $4\pi r^2 \psi(\gamma)$, we obtain

$$i = 4\pi r^2 \psi(\gamma) i_0 \left\{ \exp\left[\frac{\alpha z e}{kT}\left(\Delta E - \frac{i}{2\pi f k_e r}\right)\right] - \exp\left[-\frac{(1-\alpha) z e}{kT}\left(\Delta E - \frac{i}{2\pi f k_e r}\right)\right] \right\} \tag{9}$$

A different way of expressing the current i is to use Faraday's law, which gives the mass balance of the depositing species independently of the growth mechanism

$$i = \frac{ze}{v_m}\frac{\mathrm{d}V(t)}{\mathrm{d}t} = \frac{4\pi z e \phi(\gamma)}{v_m} r^2 \frac{\mathrm{d}r}{\mathrm{d}t} \tag{10}$$

Here $V(t)$ is the volume of the cap-shaped clusters at time t, v_m is the volume of one atom of the deposit and

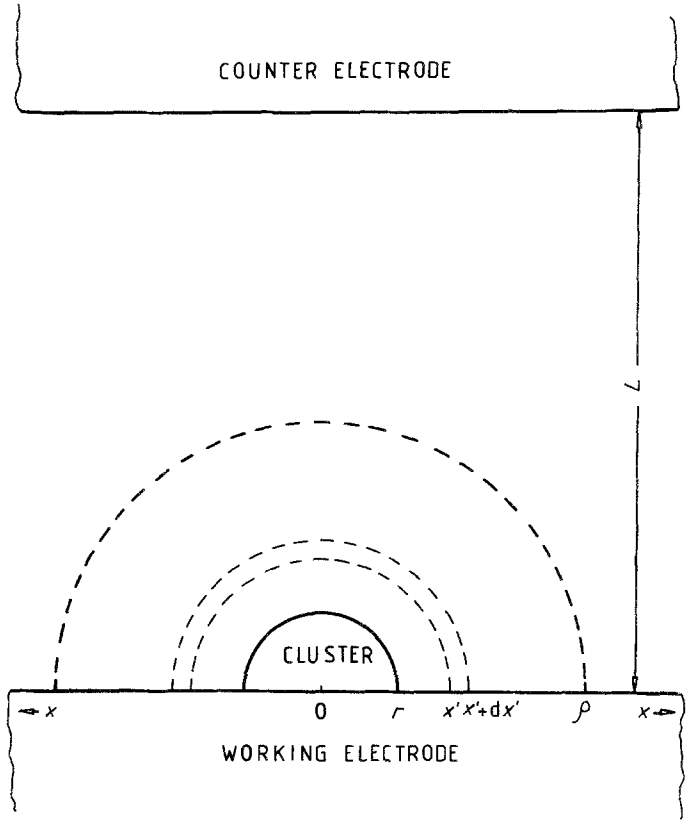

Fig. 2. Definition of the ohmic resistance of the electrolyte around a hemispherical cluster.

$\phi(\gamma) = \frac{1}{4}(2 + \cos\gamma)(1 - \cos\gamma)^2$. Equations 9 and 10 give the basic kinetic equation describing the electrochemical growth of a single cap-shaped cluster at a constant external voltage ΔE

$$\frac{dr}{dt} - P_1 \exp\left(-P_2 r \frac{dr}{dt}\right) + P_3 \exp\left(P_4 r \frac{dr}{dt}\right) = 0 \tag{11}$$

In Equation 11 the constants P_1, P_2, P_3 and P_4 read

$$P_1 = \frac{\psi(\gamma)}{\phi(\gamma) ze} v_m i_0 \exp\left(\frac{\alpha ze\Delta E}{kT}\right)$$

$$P_2 = \frac{2\alpha(ze)^2\phi(\gamma)}{f k_e v_m kT}$$

$$P_3 = \frac{\psi(\gamma)}{\phi(\gamma) ze} v_m i_0 \exp\left(-\frac{(1-\alpha) ze\Delta E}{kT}\right)$$

$$P_4 = \frac{2(1-\alpha)(ze)^2\phi(\gamma)}{f k_e v_m kT}$$

An exact analytical solution of Equation 11 is not possible, but a numerical evaluation of the $r(t)$ and $i(t)$ relationships can be carried out as follows:

(i) Using a 'zeros of function' program dr/dt is found as a function of r from Equation 11.

(ii) The plot of $(dr/dt)^{-1}$ against r is numerically integrated to give the $t(r)$ (i.e. the $r(t)$) relationship.

(iii) Having $r(t)$ and dr/dt, $i(t)$ is found from Equation 10.

The exact $r(t)$ and $i(t)$ plots obtained in this way are given by circles in Figs 3 and 4 for $v_m = 1.71 \times 10^{-23}$ cm^3 (10.28 cm^3 mol^{-1}), $i_0 = 10$ A cm^{-2}, $\alpha = 0.8$, $z = 1$, $k_e = 0.2\,\Omega^{-1}$ cm^{-1}, $T = 308$ K, $f = 1$, $\Delta E = 0.1$ V, $\gamma = 90°$ ($\psi(\gamma) = \phi(\gamma) = 0.5$). (These values correspond to electrodeposition of silver from 5 M $AgNO_3$ and are used in all numerical estimates carried out in this paper.) For comparison lines 1 in the insets (a) in Figs 3 and 4 represent the theoretical expressions for $r(t)$ and $i(t)$ obtained without taking into account the ohmic drop, that is, not introducing the term $i/2\pi k_e f r$ in Equation 9. In this case

$$r = \frac{\psi(\gamma)}{\phi(\gamma) ze} v_m i_0 \left\{\exp\left[\frac{\alpha ze\Delta E}{kT}\right] - \exp\left[-\frac{(1-\alpha) ze\Delta E}{kT}\right]\right\} t \tag{12}$$

$$i = \frac{4\pi\psi^3(\gamma)}{(ze)^2\phi^2(\gamma)} v_m^2 i_0^3 \left\{\exp\left[\frac{\alpha ze\Delta E}{kT}\right] - \exp\left[-\frac{(1-\alpha) ze\Delta E}{kT}\right]\right\}^3 t^2 \tag{13}$$

Equations 12 and 13 describe the $r(t)$ and $i(t)$ transients in the very initial stage when the interfacial ion transfer reaction is the only rate determining step. It is seen from Figs 3 and 4, however, that even for very small clusters the ohmic drop causes a significant decrease of the growth current.

In the following we derive analytical expressions for $r(t)$ and $i(t)$ accounting for the ohmic drop at short and long times, respectively.

2.1.1. Short times, low ohmic drop. In this case we rewrite Equation 9 in the form

$$i = 4\pi r^2 \psi(\gamma) i_0 \left\{\exp\left[\frac{\alpha ze\Delta E}{kT}\right] \exp\left[-\frac{\alpha ze}{2\pi f k_e kT}\frac{i}{r}\right] - \exp\left[-\frac{(1-\alpha) ze\Delta E}{kT}\right] \exp\left[\frac{(1-\alpha) ze}{2\pi f k_e kT}\frac{i}{r}\right]\right\} \tag{9'}$$

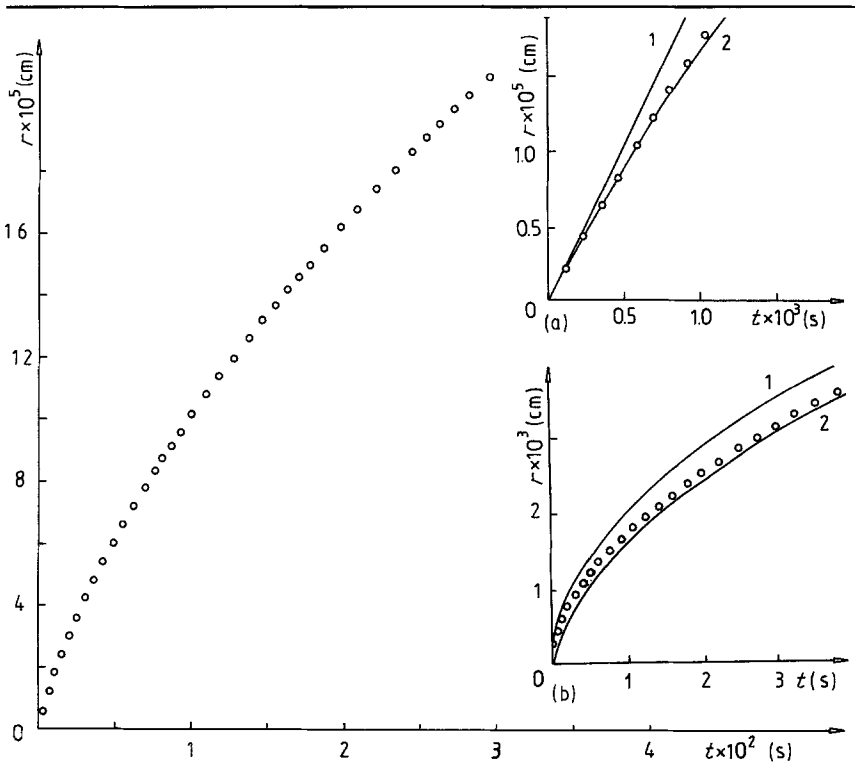

Fig. 3. Time dependence of the cluster radius r.

and express the exponents containing the ratio i/r through the first two terms of the Maclaurin expansion

$$\exp\left[-\frac{\alpha ze}{2\pi f k_e kT}\frac{i}{r}\right] \approx 1 - \frac{\alpha ze}{2\pi f k_e kT}\frac{i}{r} \quad (14)$$

$$\exp\left[\frac{(1-\alpha)ze}{2\pi f k_e kT}\frac{i}{r}\right] \approx 1 + \frac{(1-\alpha)zei}{2\pi f k_e kTr} \quad (15)$$

This is a good approximation for $(\alpha ze/2\pi f k_e kT)$ $(i/r) < 0.1$. Thus Equation 9′ simplifies to

$$i = \frac{4\pi r^2 \psi(\gamma) AkTf k_e i_0}{f k_e kT + 2\psi(\gamma) zeBi_0 r} \quad (16)$$

where

$$A = \exp\left[\frac{\alpha ze\Delta E}{kT}\right] - \exp\left[-\frac{(1-\alpha)ze\Delta E}{kT}\right]$$

$$B = \alpha \exp\left[\frac{\alpha ze\Delta E}{kT}\right] + (1-\alpha)\exp\left[-\frac{(1-\alpha)ze\Delta E}{kT}\right]$$

Combining Equations 10 and 16 yields

$$\frac{dr}{dt} = \frac{v_m A f k_e kT i_0}{zef k_e kT + 2\psi(\gamma)(ze)^2 Bi_0 r}\frac{\psi(\gamma)}{\phi(\gamma)} \quad (17)$$

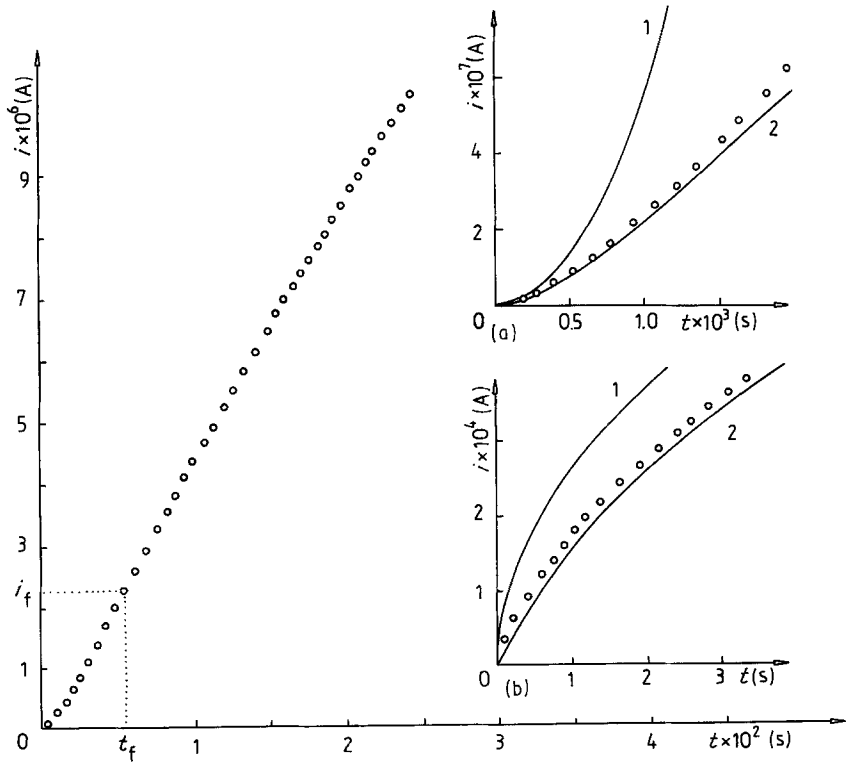

Fig. 4. Time dependence of the growth current i.

which with initial conditions $t = 0$, $r(0) = 0$, is solved to

$$r = \frac{fk_e kT}{2\psi(\gamma)zei_0 B}\left[\left(1 + \frac{4v_m i_0^2 AB\psi^2(\gamma)}{fk_e kT\phi(\gamma)}t\right)^{1/2} - 1\right] \tag{18}$$

Correspondingly, for the current i from Equations 18 and 10 (or 16), we obtain

$$i = \frac{2\pi A}{i_0\psi(\gamma)}\left(\frac{fk_e kT}{zeB}\right)^2 \times\left[\frac{1 + [2v_m i_0^2\psi^2(\gamma)ABt/\phi(\gamma)fk_e kT]}{\{1 + [4v_m i_0^2\psi^2(\gamma)ABt/\phi(\gamma)fk_e kT]\}^{1/2}} - 1\right] \tag{19}$$

Equations 18 and 19 are represented by lines 2 in the insets (a) in Figs 3 and 4 and appear to be good approximations to the exact solutions for short times when $i/r < 0.1 \times 2\pi fk_e kT/\alpha ze$. As for Equations 12 and 13 they can be used with a good accuracy if $iR_{\Omega,r}/\Delta E < 10^{-3}$.

2.1.2. Long times, high ohmic drop. At long times the external voltage ΔE is almost entirely transformed into an ohmic drop and η_r becomes low enough to justify the Maclaurin expansion of the exponents in Equation 9

$$\exp\left[\frac{\alpha ze}{kT}\left(\Delta E - \frac{i}{2\pi fk_e r}\right)\right] \approx 1 + \frac{\alpha ze}{kT}\left(\Delta E - \frac{i}{2\pi fk_e r}\right) \tag{20}$$

$$\exp\left[-\frac{(1-\alpha)ze}{kT}\left(\Delta E - \frac{i}{2\pi fk_e r}\right)\right] \approx 1 - \frac{(1-\alpha)ze}{kT}\left(\Delta E - \frac{i}{2\pi fk_e r}\right) \tag{21}$$

Thus Equation 9 simplifies to

$$i = \frac{4\pi r^2\psi(\gamma)fk_e i_0 ze\Delta E}{fk_e kT + 2\psi(\gamma)zei_0 r} \tag{22}$$

which, combined with Equation 10 yields

$$\frac{dr}{dt} = \frac{v_m fk_e i_0\Delta E}{fk_e kT + 2\psi(\gamma)zei_0 r}\frac{\psi(\gamma)}{\phi(\gamma)} \tag{23}$$

With initial conditions $t = 0$, $r(0) = 0$, the last differential equation is solved to give

$$r = \frac{fk_e kT}{2\psi(\gamma)zei_0}\left[\left(1 + \frac{4v_m i_0^2 ze\psi^2(\gamma)\Delta E}{fk_e(kT)^2\phi(\gamma)}t\right)^{1/2} - 1\right] \tag{24}$$

Correspondingly, for the current i from Equations 24 and 10 (or 22) we obtain

$$i = \frac{2\pi f^2 k_e^2 kT\Delta E}{\psi(\gamma)zei_0}\left[\frac{1 + [2v_m i_0^2\psi^2(\gamma)ze\Delta Et/\phi(\gamma)fk_e(kT)^2]}{\{1 + [4v_m i_0^2\psi^2(\gamma)ze\Delta Et/\phi(\gamma)fk_e(kT)^2]\}^{1/2}} - 1\right] \tag{25}$$

Equation 24 and 25 are represented by lines 2 in the insets (b) in Figs 3 and 4 and are good approximations to the exact solutions for long times when $i/r > 2\pi fk_e(\Delta E - 0.1kT/\alpha ze)$.

Finally, lines 1 in the insets (b) in Figs 3 and 4 represent the limiting case of complete ohmic control of the growth process [2] when the whole external voltage ΔE is transformed into an ohmic drop ($\eta_r = 0$)

$$\Delta E = \frac{i}{2\pi fk_e r} \tag{26}$$

In this case combining Equations 26 and 10 and solving the differential equation with initial conditions $t = 0$, $r(0) = 0$ yields [2]

$$r = [fk_e v_m\Delta E/ze\phi(\gamma)]^{1/2}t^{1/2} \tag{27}$$

$$i = 2\pi(fk_e\Delta E)^{3/2}[v_m/ze\phi(\gamma)]^{1/2}t^{1/2} \tag{28}$$

The expressions 27 and 28 follow also from Equations 24 and 25 for sufficiently long times when $[v_m i_0^2 ze\psi^2(\gamma)\Delta Et/fk_e\phi(\gamma)(kT)^2] \gg 1$.

2.2. *Interpretation of the experimental results*

The previous considerations illustrate the influence of the ohmic drop on the $r(t)$ and $i(t)$ behaviour of a small cap-shaped cluster of the new phase. As is seen from Fig. 4 characteristic feature of the current transient is its inflection point appearing at time $t = t_f$ ($i = i_f$) as a result of the gradual transition from the i–t^2 time law (complete "ion transfer control" Equation 13) to the i–$t^{1/2}$ time law (complete 'ohmic' control, Equation 28). As mentioned in the previous section an exact analytical expression for the $i(t)$ relationship cannot be obtained and this makes the direct quantitative interpretation of an experimental current transient impossible. However, information about the kinetic parameters of the growth process can be derived from the approximate solutions for $i(t)$, valid at short and long times respectively (Equations 19 and 25).

Applying the condition for inflection $[d^2i/dt^2]_{t=t_f} = 0$ to Equation 19 for the coordinates of the inflection point one obtains

$$t_{f,s} = \frac{fk_e kT\phi(\gamma)}{2v_m i_0^2\psi^2(\gamma)AB} \tag{29}$$

$$i_{f,s} = \frac{2 - 3^{1/2}}{3^{1/2}}\frac{2\pi A}{i_0\psi(\gamma)}\left(\frac{fk_e kT}{zeB}\right)^2 \tag{29'}$$

whereas from Equation 25 we obtain

$$t_{f,l} = \frac{fk_e(kT)^2\phi(\gamma)}{2v_m i_0^2\psi^2(\gamma)ze\Delta E} \tag{30}$$

$$i_{f,l} = \frac{2 - 3^{1/2}}{3^{1/2}}\frac{2\pi(fk_e)^2 kT\Delta E}{\psi(\gamma)i_0 ze} \tag{30'}$$

These two sets of kinetic formulae can be used to evaluate i_0 and fk_e approximately from the coordinates of the inflection point of an experimental current transient if the wetting angle, γ, is known. In order to indicate the accuracy of such an estimate let us

assume that the exact $i(t)$ plot (the circles in Fig. 4) is an experimental transient with inflection at time $t_f = 5.51 \times 10^{-3}$ s ($i_f = 2.28 \times 10^{-6}$ A). Then Equations 29 and 29′ give $i_0 = 7.6\,\mathrm{A\,cm^{-2}}$ and $fk_e = 0.41\,\Omega^{-1}\,\mathrm{cm^{-1}}$, whereas Equations 30 and 30′ give $i_0 = 27.4\,\mathrm{A\,cm^{-2}}$ and $fk_e = 0.11\,\Omega^{-1}\,\mathrm{cm^{-1}}$. These values of fk_e and i_0 do not differ dramatically from the true values ($fk_e = 0.2\,\Omega^{-1}\,\mathrm{cm^{-1}}$ and $i_0 = 10\,\mathrm{A\,cm^{-2}}$) used to obtain the exact $i(t)$ plot given in Fig. 4. However, if a more accurate estimate is needed an appropriate choice between the two sets of formulae for i_f and t_f (Equations 29, 29′ and 30, 30′) should be made by checking which of the two inequalities

$$\frac{i_f}{r_f} < 0.1 \times 2\pi f k_e kT/\alpha z e \quad \text{(short-time approximation)}$$

or

$$\frac{i_f}{r_f} > 2\pi f k_e(\Delta E - 0.1kT/\alpha z e)$$

(long-time approximation)

holds for the experimental inflection point. For this purpose it is also necessary to find the radius r_f of the cluster at time $t = t_f$. This can be easily done by integrating the experimental current transient and determining the $r(t)$ relationship according to Faraday's law (Equation 10)

$$r(t) = \left[\frac{3v_m}{4\pi z e \phi(\gamma)} \int_0^t i(t)\,\mathrm{d}t\right]^{1/3} \tag{31}$$

Of course, having data for $i(t)$ and $r(t)$, a direct interpretation is also possible on the basis of the general Equation 8 presented in the form $i/r^2 = F(i/r)$. Using a 'best fit' procedure one can determine i_0, f and $\psi(\gamma)$ at given α, T and k_e.

Finally, let us consider two experimental current transients corresponding to the growth of hemispherical ($\alpha = 90°$, $\phi(\gamma) = \psi(\gamma) = 0.5$) silver and lead single crystals from 5 M $AgNO_3$ and 0.5 M $Pb(NO_3)_2$ respectively (Fig. 5a and b) [2]. The other parameters for these experiments are $\Delta E = 0.01$ V, $T = 310$ K and $k_e = 0.21\,\Omega^{-1}\,\mathrm{cm^{-1}}$ for silver and $\Delta E = 0.004$ V, $T = 295$ K and $k_e = 0.058\,\Omega^{-1}\,\mathrm{cm^{-1}}$ for lead electrodeposition. Integrating the current transients and calculating the cluster radius according to Equation 31 for the ratios i/r give

$$\frac{i}{r} \geqslant 1.31 \times 10^{-2}\,\mathrm{A\,cm^{-1}} \text{ for } t \geqslant 25\,\mathrm{s} \text{ (silver)}$$

$$\frac{i}{r} \geqslant 1.55 \times 10^{-3}\,\mathrm{A\,cm^{-1}} \text{ for } t \geqslant 120\,\mathrm{s} \text{ (lead)}$$

In both cases this justifies the use of the long-time approximation (Equation 25) for interpretation of the experimental results. The i against $t^{1/2}$ plots given in Figs 6a and b show that at long times the data satisfy a linear relationship of the type

$$i = at^{1/2} + b \tag{32}$$

where $a = 1.06 \times 10^{-5}\,\mathrm{A\,s^{-1/2}}$, $b = -2.5 \times 10^{-5}$ A for silver and $a = 4 \times 10^{-7}\,\mathrm{A\,s^{-1/2}}$, $b = 1.8 \times 10^{-6}$ A for lead electrodeposition. It can readily be shown that such a current-time law follows directly from Equation 25 if two inequalities are simultaneously fulfilled

$$\frac{2v_m i_0^2 z e \Delta E \psi^2(\gamma)}{f k_e (kT)^2 \phi(\gamma)}\, t \geqslant 10 \tag{33}$$

$$\left[\frac{v_m i_0^2 z e \Delta E \psi^2(\gamma)}{2 f k_e (kT)^2 \phi(\gamma)}\, t\right]^{1/2} < 10 \tag{33′}$$

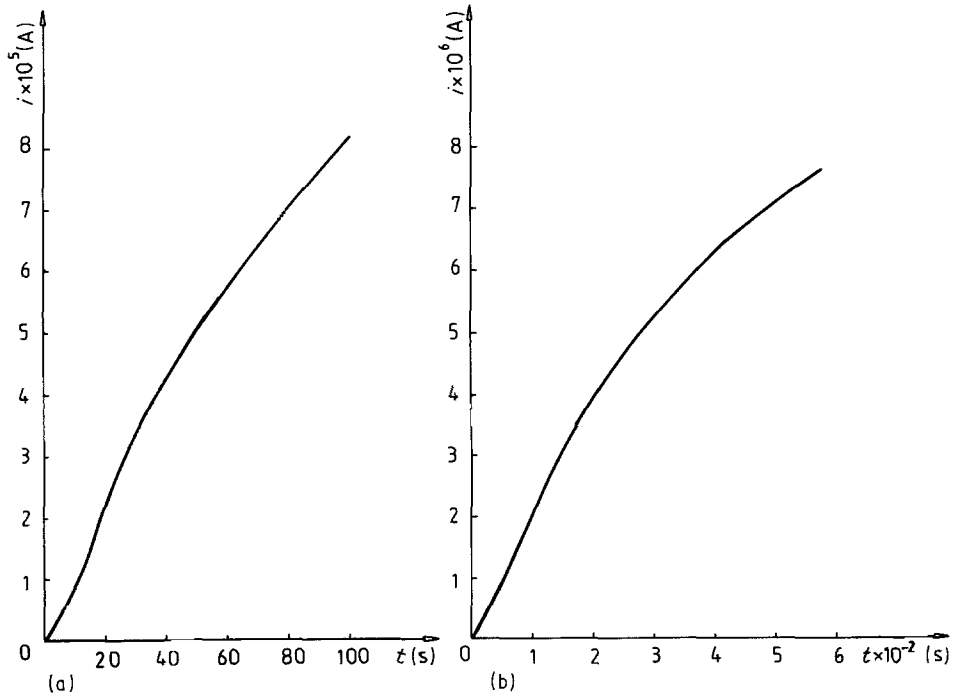

Fig. 5. Growth current of hemispherical (a) silver and (b) lead single crystals in 5 M $AgNO_3$ and 0.5 M $Pb(NO_3)_2$ (according to [2]).

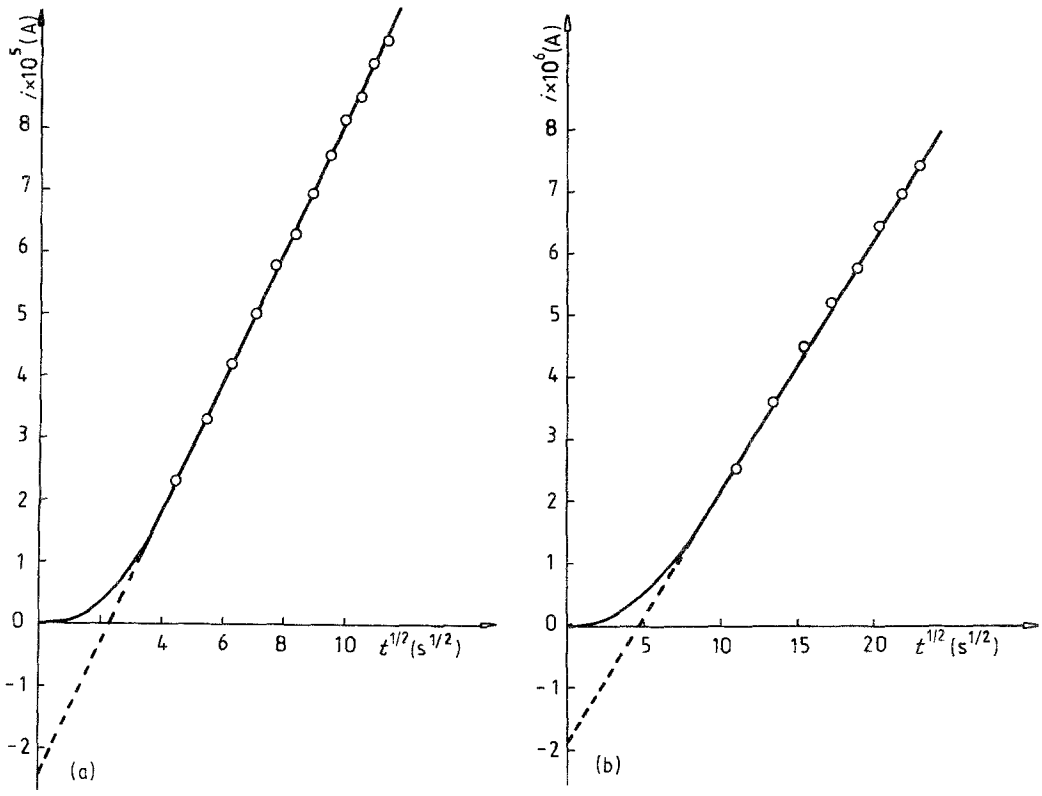

Fig. 6. Plots of i against $t^{1/2}$ for the data from Fig. 5.

In this case for the time interval $\Delta t = 190 f k_e (kT)^2 \phi(\gamma)/v_m i_0^2 ze\Delta E \psi^2(\gamma)$, Equation 25 simplifies to

$$i = 2\pi(f k_e \Delta E)^{3/2}[v_m/ze\phi(\gamma)]^{1/2} t^{1/2} - 2\pi(f k_e)^2 kT\Delta E/\psi(\gamma) i_0 ze \qquad (34)$$

which allows calculation of $f k_e$ from the slope and i_0 from the intercept of an experimental i against $t^{1/2}$ transient. In the cases under consideration the values obtained are $f k_e = 0.24\,\Omega^{-1}\,\mathrm{cm}^{-1}$, $i_0 = 7.6\,\mathrm{A\,cm}^{-2}$ for silver and $f k_e = 0.069\,\Omega^{-1}\,\mathrm{cm}^{-1}$, $i_0 = 1.7\,\mathrm{A\,cm}^{-2}$ for lead electrodeposition. Of course, it should not be forgotten that, for crystalline clusters, each crystallographic face is characterized by a different exchange current density. Therefore the above values of i_0 have to be considered as mean values reflecting the specific crystallographic relief of the silver and the lead single crystals at the given experimental conditions.

An important point in the theoretical interpretation of the experimental results is the determination of the constant f. In the above cases the comparison between the product $f k_e$ and the corresponding bulk conductivities k_e yields $f = 1.14$ for silver and $f = 1.19$ for lead electrodeposition. This means that for hemispherical clusters f is probably rather close to unity. In the case of an arbitrary contact angle ($\gamma \neq 90°$), however, f has to be experimentally determined by studying the growth kinetics at long times and interpreting the $r(t)$ and $i(t)$ transients by means of Equations 27 and 28. Knowing the values of γ and k_e, f can readily

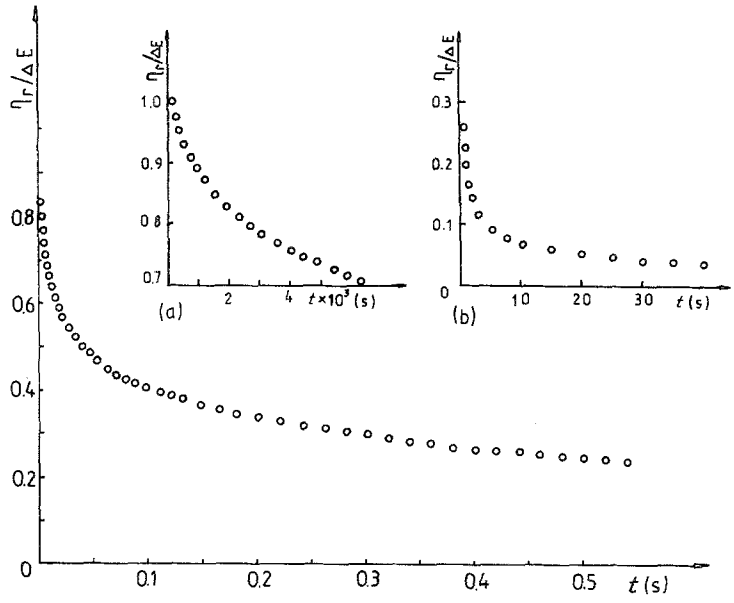

Fig. 7. Dimensionless plot of $\eta_r/\Delta E$ against t calculated according to Equation 35 with the exact $r(t)$ and $i(t)$ relationships (circles in Figs 3 and 4 respectively). Insets (a) and (b) — short and long times respectively.

be found from the slope of the r against $t^{1/2}$ (or i against $t^{1/2}$) experimental plot.

2.3. *Zones of reduced overpotential*

As pointed out at the beginning of this study the appearance of a growing cluster on the electrode surface leads to a local decrease in the overpotential, η, and modifies the electric field in the cluster vicinity. We have already seen that at the cluster surface (at a distance $x = r$, Fig. 2) the overpotential of the double layer is

$$\eta_r = \Delta E - iR_{\Omega,r} = \Delta E\left(1 - \frac{i}{2\pi f k_e r \Delta E}\right) \quad (35)$$

where $R_{\Omega,r} = 1/2\pi f k_e r$ is the total ohmic resistance of the circuit 'counter electrode–electrolyte–r-sized growing cluster' and the current i is given by Equations 9 or 10. Knowing the $r(t)$ and the $i(t)$ relationships (Figs 3 and 4) Equation 35 allows calculation of the time dependence of the overpotential at the cluster surface. The latter is given in Fig. 7 in dimensionless units $\eta_r/\Delta E$ against t.

An important problem in electrochemical phase formation is the determination of the overpotential distribution around a growing stable cluster. This involved determining the overpotential as a function of the distance x from the cluster surface. To achieve this it is necessary to take into account, not the total ohmic drop, $iR_{\Omega,r}$, but only that part of it due to the ohmic resistance R_ϱ of the electrolyte between the counter electrode and the imaginary hemisphere of radius ϱ (Fig. 2). Since R_ϱ is given by

$$R_\varrho = \int_{f_\rho}^{L} \frac{dx'}{2\pi k_e x'^2} \quad (36)$$

the resulting expression for η_ϱ is

$$\eta_\varrho = \Delta E - i\int_{f_\rho}^{L} \frac{dx'}{2\pi k_e x'^2} \quad (37)$$

Therefore, assuming that the counter electrode is infinitely large and infinitely distant ($L \gg \varrho$), one finally obtains

$$\eta_\varrho = \Delta E - \frac{i}{2\pi f k_e \varrho}\left(1 - \frac{f\varrho}{L}\right) \approx \Delta E\left(1 - \frac{i}{2\pi f k_e \varrho \Delta E}\right) \quad (38)$$

It is seen from this expression that, for $\varrho = r$, the overpotential η_ϱ equals η_r (Equation 35) whereas for $\varrho \to \infty$, that is, at sufficiently long distance from the cluster, η_ϱ attains the value of the external voltage ΔE.

Figure 8 shows the cross section of six overpotential profiles drawn on the basis of Equation 38. Each profile relates to a different time t, that is, to a different current $i(t)$ and cluster radius $r(t)$. The length of the horizontal part of each profile equals the cluster diameter, whereas its ordinate gives the ratio $\eta_\varrho/\Delta E$ at the cluster surface ($\varrho = r$). Combining Equations 35 and 38 yields

$$\eta_\varrho = \eta_r + \frac{i}{2\pi f k_e}\left(\frac{1}{r} - \frac{1}{\varrho}\right) \quad (39)$$

which directly illustrates the interrelation between the overpotentials η_ϱ and η_r. Making use of Equation 38 one can also determine the radius ϱ of the zone of reduced overpotential

$$\varrho = \frac{i}{2\pi f k_e(\Delta E - \eta_\varrho)} \quad (40)$$

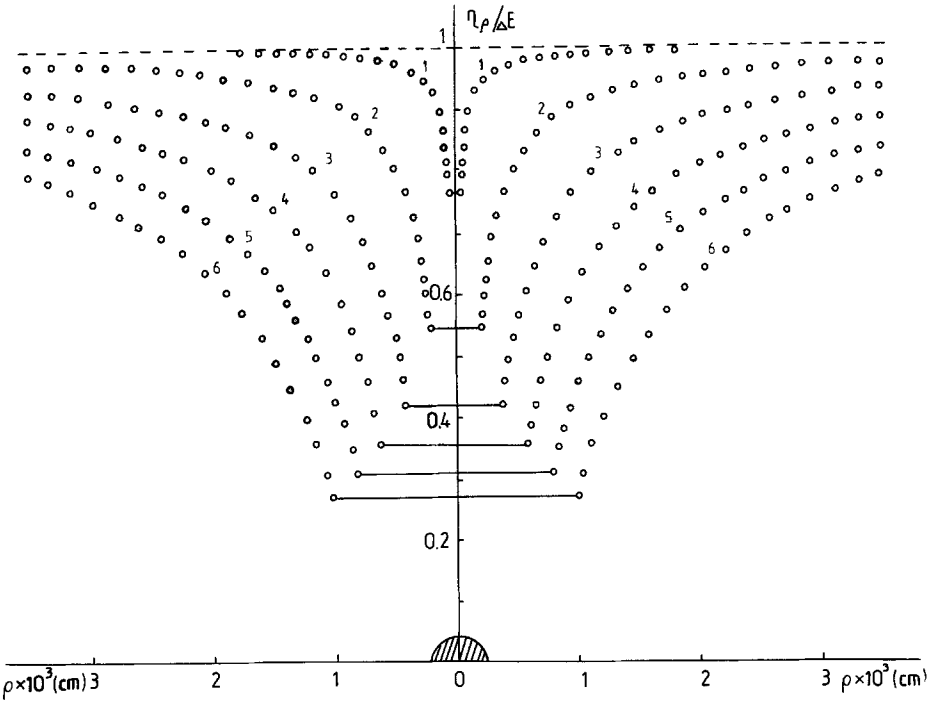

Fig. 8. Overpotential profiles around a growing hemispherical cluster. 1: $t = 0.38 \times 10^{-2}$ s, $r = 5 \times 10^{-5}$ cm, $i = 1.48 \times 10^{-6}$ A; 2: $t = 2.70 \times 10^{-2}$ s, $r = 2 \times 10^{-4}$ cm, $i = 1.12 \times 10^{-5}$ A; 3: $t = 8.1 \times 10^{-2}$ s, $r = 4 \times 10^{-4}$ cm, $i = 2.91 \times 10^{-5}$ A; 4: $t = 16.6 \times 10^{-2}$ s, $r = 6 \times 10^{-4}$ cm, $i = 4.86 \times 10^{-5}$ A; 5: $t = 27 \times 10^{-2}$ s, $r = 8 \times 10^{-4}$ cm, $i = 6.96 \times 10^{-5}$ A; 6: $t = 40 \times 10^{-2}$ s, $r = 1 \times 10^{-3}$ cm, $i = 9.15 \times 10^{-5}$ A.

in which η varies from η_r at the cluster surface to η_ϱ at the zone periphery. Putting η_ϱ equal to the 'critical' nucleation overpotential, η_c, one obtains from Equation 40 the radius ϱ_c of the so called 'nucleation exclusion zone' in which no nuclei form under given experimental conditions. However, the critical overpotential η_c is not a thermodynammic quantity. It is defined as the overpotential at which the nucleation rate equals one nucleus per unit time and depends on the properties of the particular experimental system. Equation 40 shows that, apart from the constant factor $[2\pi f k_e(\Delta E - \eta_\varrho)]^{-1}$, the time dependence of the zone radius ϱ coincides with the time dependence of the growth current i (Fig. 4). However, one should bear in mind that Equation 40 only holds for values of η_ϱ greater than, or equal to η_r and the zone radius ϱ is in all cases greater than, or equal to, the cluster radius r. The interrelation between ϱ and r is revealed by substituting Faraday's law (Equation 10) into Equation 40. The result obtained is

$$\varrho = \frac{2ze\phi(\gamma)}{v_m f k_e(\Delta E - \eta_\varrho)} r^2 \frac{dr}{dt} \tag{41}$$

Only in the limiting case of complete ohmic control of the growth of hemispherical clusters from Equations 26 and 40 can one obtain the simple formula suggested by Markov *et al.* [6]

$$\varrho = \frac{\Delta E}{\Delta E - \eta_\varrho} r \tag{42}$$

Rearrangement of Equation 42 yields

$$\eta_\varrho = \Delta E \left(1 - \frac{r}{\varrho}\right) \tag{42'}$$

which gives the overpotential profile arising around a growing macrocluster after a sufficiently long time when the external voltage is entirely compensated by the ohmic drop. In this case, for the cluster surface ($\varrho = r$), Equation 42' gives $\eta_\varrho/\Delta E = 0$. However, a numerical estimate based on the exact formulae of Equations 10, 11 and 35 shows that η_r differs from zero even for rather long times. Thus $\eta_\varrho/\Delta E = 0.05$ at $t = 30$ s ($r = 1.08 \times 10^{-2}$ cm, $i = 1.30 \times 10^{-3}$ A). In fact these values of t, r and i may be considered as lower limits for the validity of the theoretical formulae derived for the case of complete ohmic control of the growth process (Equations 27, 28, 42 and 42'). Of course, the estimate relates to the particular numerical values of the physical quantities used in this study.

The profile 3 in Fig. 9 represents Equation 42' in dimensionless coordinates $\eta_\varrho/\Delta E$ against ϱ/r. For comparison profiles 1 and 2 represent the exact solution (Equation 38) for clusters of sizes $r = 5 \times 10^{-5}$ cm and $r = 6 \times 10^{-4}$ cm respectively. (Profiles 1 and 2 in Fig. 9 correspond to profiles 1 and 4 in Fig. 8.) As is seen from Fig. 9, the simple formulae Equations 42 and 42' do not provide a satisfactory description of the overpotential distribution at short times when the nucleation phenomena normally take place. For example, for $r = 5 \times 10^{-5}$ cm the exact solution (line 1, Fig. 9) shows that the overpotential, η_ϱ, attains the value $0.95\Delta E$ at a distance $\varrho = 5r$, whereas Equation 42' predicts $\eta_\varrho = 0.95\Delta E$ at $\varrho = 20r$. The corresponding zone surface area, $S_\varrho = \pi\varrho^2$, are $25\pi r^2$ and $400\pi r^2$, respectively. This means that misleading information would be obtained if nucleation experiments are interpreted by assuming that the clusters grow under the conditions of complete 'ohmic' control from the very beginning of the deposition process. Of course, if the zones of reduced overpoten-

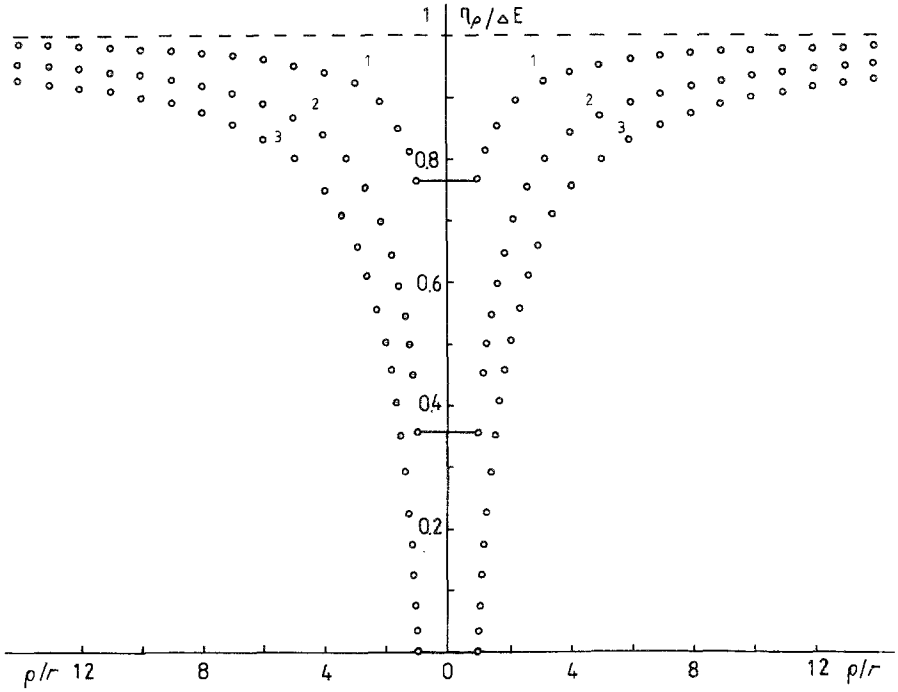

Fig. 9. Dimensionless plots of $\eta_\varrho/\Delta E$ against ϱ/r calculated according to Equation 38 (lines 1 and 2) and according to Equation 42' (line 3).

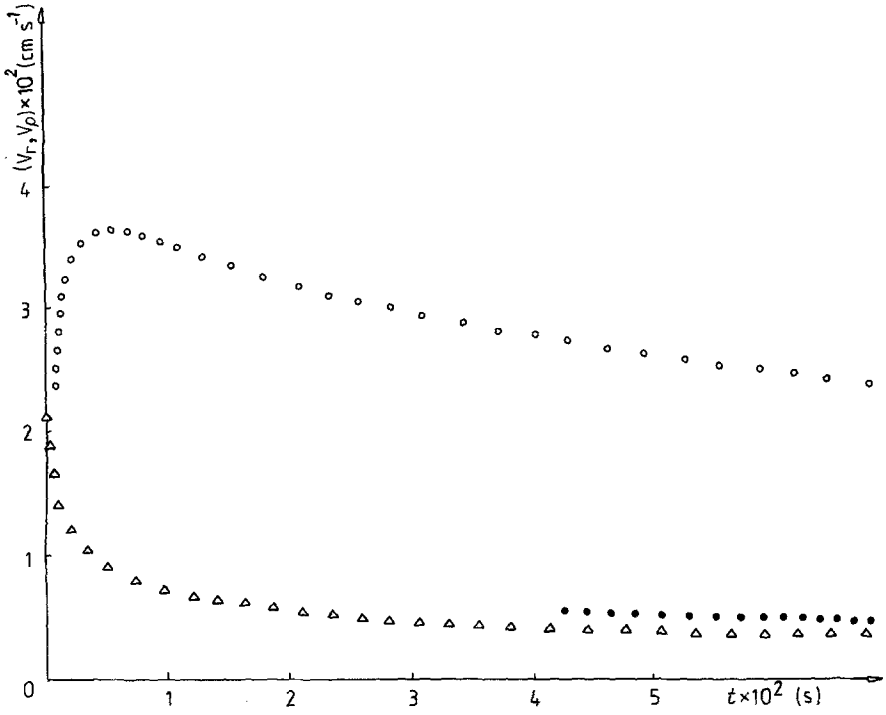

Fig. 10. Time dependence of the growth rates v_r (△) and v_ϱ (○) for $\eta_\varrho = 0.5\Delta E$ and (●) for $\eta_\varrho = 0.9\Delta E$.

tial are totally neglected wrong results would also be obtained.

An important characteristic of the zones of reduced overpotential is their rate of spread. Two quantities can, in principle, be defined: the growth rate of the zone radius, $v_\varrho = \mathrm{d}\varrho/\mathrm{d}t$, and the growth rate of the zone surface area, $V_\varrho = \mathrm{d}S_\varrho/\mathrm{d}t$. The connection between v_ϱ, V_ϱ and the corresponding cluster growth rates, v_r and V_r, is found by means of Equation 41

$$v_\varrho = \frac{2ze\phi(\gamma)}{fk_e v_m(\Delta E - \eta_\varrho)}\left(2rv_r^2 + r^2\frac{\mathrm{d}v_r}{\mathrm{d}t}\right) \quad (43)$$

$$V_\varrho = \left[\frac{ze}{8\pi v_m fk_e(\Delta E - \eta_\varrho)}\right]^2 \frac{\phi^2(\gamma)}{\psi^3(\gamma)}\left(V_r^3 + 2S_r V_r \frac{\mathrm{d}V_r}{\mathrm{d}t}\right) \quad (44)$$

The time dependence of the quantity v_r is given by triangles in Fig. 10. As is seen it has a non-zero initial value corresponding to the case of complete 'ion transfer' control (Equation 12)

$$v_0 = \left(\frac{\mathrm{d}r}{\mathrm{d}t}\right)_{t=0} = \frac{\psi(\gamma)}{ze\phi(\gamma)} v_m i_0 \left\{\exp\left[\frac{\alpha ze\Delta E}{kT}\right] - \exp\left[-\frac{(1-\alpha)ze\Delta E}{kT}\right]\right\} \quad (45)$$

and tends to zero at long times when the clusters grow under the conditions of complete 'ohmic' control (Equation 27)

$$v_\infty = \left(\frac{\mathrm{d}r}{\mathrm{d}t}\right)_{t\to\infty} = [fk_e v_m \Delta E/4ze\phi(\gamma)]^{1/2} t^{-1/2} \quad (46)$$

The open and solid circles in Fig. 10 represent the time dependence of the rate, v_ϱ, of spread of two zones of reduced overpotential – the one corresponding to $\eta_\varrho = 0.5\Delta E$ and the other corresponding to $\eta_\varrho = 0.9\Delta E$. The significant difference in the two relationships is due to the different times of the appearance of the zones. Thus the zone corresponding to $\eta_\varrho = 0.5\Delta E$ arises after time $t^* = 4.23 \times 10^{-2}$ s from the cluster formation at $t = 0$. Since the time t^* is well after the inflection point of the $i(t)$ relationship ($t_f = 5.51 \times 10^{-3}$ s) the function $v_\varrho = \mathrm{d}\varrho/\mathrm{d}t \approx \mathrm{d}i/\mathrm{d}T$ (Equation 40) decreases monotonically. The zone corresponding to $\eta_\varrho = 0.9\Delta E$ arises at time $t^* = 8.95 \times 10^{-4}$ s and its rate of spread displays a maximum at $t = t_f$. The quantity V_r (Fig. 11) increases with time from zero (at $t = 0$) to the constant value $V_{r,\infty} = [8\pi\psi(\gamma)v_m fk_e\Delta E/ze]$ at $t \to \infty$. The corresponding zone growth rate

$$V_\varrho = 4\pi\varrho\frac{\mathrm{d}\varrho}{\mathrm{d}t} = \frac{4\pi}{[2\pi fk_e(\Delta E - \eta_\varrho)]^2} i\frac{\mathrm{d}i}{\mathrm{d}t} \quad (47)$$

are also increasing functions of time in the interval (0 to 7×10^{-2} s). However, a simple inspection of Equation 47, based on the approximate analytical solutions for i (Equations 19 and 25), shows that V_ϱ displays a maximum at time $t_{m(s,l)} = \frac{3}{2}t_{f(s,l)}$ and tends to the constant value $V_{\varrho,\infty} = \pi fk_e\Delta E^3 v_m/ze\phi(\gamma)(\Delta E - \eta_\varrho)^2$ at $t \to \infty$ when the clusters grow under the conditions of complete 'ohmic' control.

The results obtained in this section illustrate the complicated kinetics of spread of the zones of reduced overpotential. In particular, the examination of the quantity v_ϱ indicates that the simple power law $v_\varrho \sim t^n$ suggested by Markov [16] could hardly be applied to the initial stage of the phase formation. This also makes questionable the interpretation of the experimental results carried out in [17–20].

3. Conclusions

The theoretical analysis performed in this study

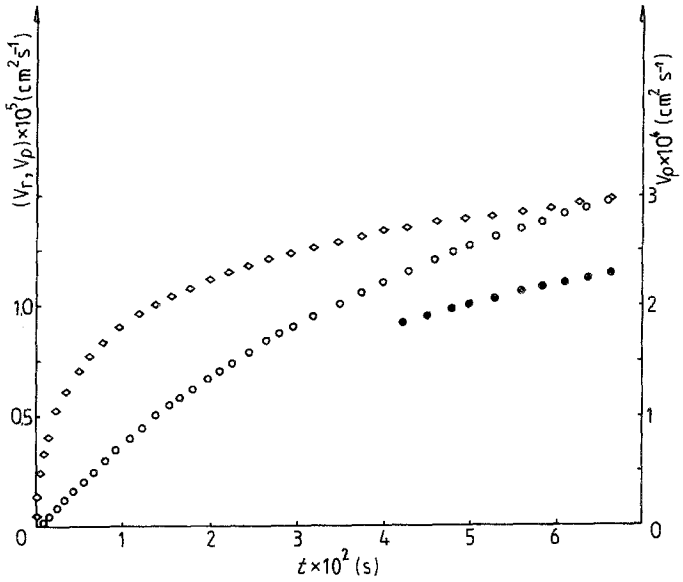

Fig. 11. Time dependence of the growth rates V_r (◇) and V_ϱ (○) for $\eta_\varrho = 0.5\Delta E$ and (●) for $\eta_\varrho = 0.9\Delta E$ (right-hand-side ordinate).

unambiguously shows that under certain experimental conditions the ohmic drop may play a significant role in the electrodeposition process and this should be borne in mind even when interpreting the growth kinetics of very small clusters. On increasing the cluster size the ohmic effects become more and more important, thus leading to the establishment of a complete ohmic control of the growth process. The last limiting case was first considered by Scheludko and Bliznakov [2]. In a recent paper, Deutscher and Fletcher [21] comment upon the theory developed in [2], arguing that 'it fails to describe real data', but is expected to hold 'only in the most extreme cases'. It is our opinion that this criticism is somewhat exaggerated. On one hand, the exchange current densities (10^{-3} to 10^{-18} A cm^{-2}), which the authors of [21] use to estimate the ion transfer resistance $R_{i,t}$, are rather low and reflect by no means the vast majority of the 'metal–metal ion' reactions. Much higher values of i_0 were found for many electrochemical systems quite a long time ago. Thus for the Hg/Hg^{2+} electrode Gerischer [22] has found $i_0 = 5\,A\,cm^{-2}$ (see also [23, 24]), whereas for the Ag/Ag^+ electrode i_0 was found to vary from 0.15 to 4.5 A cm^{-2} [25] and from 1 to 7 A cm^{-2} [26] (see also [27]). Relatively high values for i_0 (~ 0.1 A cm^{-2}) were also reported for many amalgam electrodes [28] and much higher exchange current densities (~ 500 A cm^{-2}) were measured in fused salts [4]. All these data show that the ion transfer resistance, $R_{i,t}$, which is generally inversely proportional to i_0, does not always have a very high value and could be

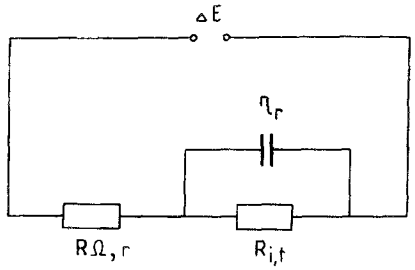

Fig. 12. Equivalent scheme of the electrochemical circuit 'counter electrode–electrolyte–r-sized cluster'.

commensurate with the ohmic resistance $R_{\Omega,r}$. On the other hand it is well known that the expression which Deutscher and Fletcher use to evaluate the ion transfer resistance ($R_{i,t} = vkT/i_0ze$) and to compare it with $R_{\Omega,r}$ holds only for low overpotentials, η, and/or high temperatures, T, when $ze\eta/kT \ll 1$. In our opinion the correct comparison between $R_{\Omega,r}$ and $R_{i,t}$ (measured in Ω not in Ω cm^2) should be carried out in the following way.

The equivalent scheme of the electrochemical circuit 'counter electrode–electrolyte–r-sized growing cluster' is shown in Fig. 12. According to this scheme the growth current, i, is given by

$$i = \frac{\Delta E}{R_{i,t} + R_{\Omega,r}} \tag{48}$$

Hence for $R_{i,t}$

$$R_{i,t} = \frac{\Delta E}{i} - \frac{1}{2\pi f k r_e} \tag{49}$$

The resistances $R_{i,t}$, $R_{\Omega,r}$ and the total resistance $R_T = R_{it} + R_{\Omega,r}$ are calculated as functions of the cluster radius r and are shown in double logarithmic coordinates in Fig. 13. As is seen, for small clusters the total resistance (line 1) is almost equal to the ion transfer resistance $R_{i,t}$ (line 2). For sufficiently large clusters R_T is close to $R_{\Omega,r}$ (line 3). The exact lowest and highest calculated values of $R_{\Omega,r}$, $R_{i,t}$ and R_T are:

for $r = 2 \times 10^{-6}$ cm, $i = 4.71 \times 10^{-9}$ A

$R_{i,t} = 2.08 \times 10^7\,\Omega$, $R_{\Omega,r} = 3.98 \times 10^5\,\Omega$,

$R_T = 2.12 \times 10^7\,\Omega$

for $r = 6.9 \times 10^{-3}$ cm, $i = 8.09 \times 10^{-4}$ A

$R_{i,t} = 8.18\,\Omega$, $R_{\Omega,r} = 1.15 \times 10^2\,\Omega$,

$R_T = 1.2 \times 10^2\,\Omega$

These numerical estimates show that in the advanced stage of the deposition process the growth proceeds under complete ohmic control. For smaller clusters, however, both ohmic and ion transfer limitations have to be taken into consideration.

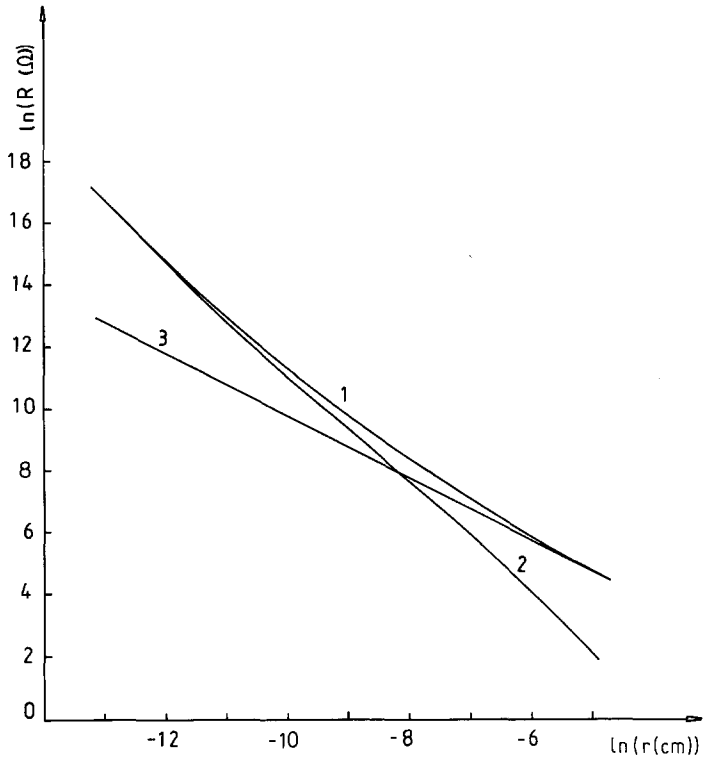

Fig. 13. Plots of the resistances R_T (1), $R_{i,t}$ (2) and $R_{\Omega,r}$ (3) against the cluster radius r.

Acknowledgements

This project was completed with the financial support of the Committee of Science at the Council of Ministers under contract No. KH 168, 1987. The author thanks Dr V. Tsakova for the computer program.

References

[1] J. Malinovski and E. Budevski, *Izv. Bulg. Akad. Nauk.* **2** (1951) 205.
[2] A. Scheludko and G. Bliznakov, *ibid.* **2** (1951) 239.
[3] M. Fleischmann and H. R. Thirsk, in 'Advances in Electrochemistry and Electrochemical Engineering' (edited by P. Delahay), Vol. III, Wiley, New York (1963) Chap. 3.
[4] A. N. Baraboshkin, L. T. Kosikhin and N. A. Saltykova, *Trudy Inst. Elektrokhimii Uralsk, Filial Akad. Nauk. USSR* **7** (1965) 47.
[5] D. J. Astley, J. A. Harrison and H. R. Thirsk, *Trans. Farad. Soc.* **64** (1968) 192.
[6] I. Markov, A. Boynov and S. Toschev, *Electrochim. Acta* **18** (1973) 377.
[7] D. Kashchiev and A. Milchev, *Thin Solid Films* **28** (1975) 189,201.
[8] B. Scharifker and G. Hills, *J. Electroanal. Chem.* **130** (1981) 81.
[9] A. Milchev, B. Scharifker and G. Hills, *ibid.* **132** (1982) 277.
[10] E. Bosko and S. K. Rangarajan, *ibid.* **134** (1982) 213.
[11] S. Fletcher, *J.C.S. Faraday. Trans.I* **79** (1983) 467.
[12] M. Y. Abyaneh, *J. Electroanal. Chem.* **209** (1986) 1.
[13] R. Kaischev and D. Kashchiev, Proceedings of the 28th ISE Meeting, Varna, Ext. Abst. Vol. I, p. 63.
[14] J. M. Polukarov and A. I. Danilov, *Elektrokhimia* **17** (1981) 1883.
[15] W. Lorenz, *Z. Phys. Chem.* **202** (1953) 275.
[16] I. Markov, *Thin Solid Films* **35** (1976) 11.
[17] I. Markov and E. Stoycheva, *ibid.* **35** (1976) 21.
[18] V. V. Trofimenko, V. P. Zhitnik and Ju. M. Loschkarev, *Elektrokhimia* **15** (1979) 1035.
[19] V. V. Trofimenko, V. P. Zhitnik, T. G. Aleksandrova and Ju. M. Loschkarev, *ibid.* **16** (1980) 1139.
[20] V. V. Trofimenko, V. P. Zhitnik and Ju. M. Loschkarev, *ibid.* **17** (1981) 1644.
[21] R. L. Deutscher and S. Fletcher, *J. Electroanal. Chem.* **239** (1988) 17.
[22] H. Gerischer, *Z. Electrochem.* **55** (1951) 98.
[23] H. Gerischer and M. Krauze, *Z. Phys. Chem.* (*N.F.*) **10** (1957) 264.
[24] *Idem, ibid.* **14** (1958) 184.
[25] H. Gerischer and R. P. Tischer, *Z. Elektrochem.* **61** (1957) 1159.
[26] P. B. Price and D. A. Vermilyea, *J. Chem. Phys.* **28** (1958) 720.
[27] T. Vitanov, A. Popov and E. Budevski, *J. Electrochem. Soc.* **121** (1974) 207.
[28] K. J. Vetter, in 'Elektrochemische Kinetik', Springer, Berlin (1961).
[29] V. Bostanov, R. Rusinova and E. Budevski, *Commun. Dept. Chem. Bulg. Acad. Sci.* **2** (1969) 885.